

Revisit of constraints on holographic dark energy: SNLS3 dataset with the effects of time-varying β and different light-curve fitters

Shuang Wang,¹ Jia-Jia Geng,¹ Yi-Liang Hu,¹ and Xin Zhang^{*1, 2, †}

¹*Department of Physics, College of Sciences, Northeastern University, Shenyang 110004, China*

²*Center for High Energy Physics, Peking University, Beijing 100080, China*

Previous studies have shown that for the Supernova Legacy Survey three-year (SNLS3) data there is strong evidence for the redshift-evolution of color-luminosity parameter β of type Ia supernovae (SN Ia). In this paper, we explore the effects of varying β on the cosmological constraints of holographic dark energy (HDE) model. In addition to the SNLS3 data, we also use Planck distance prior data of cosmic microwave background (CMB), as well as galaxy clustering (GC) data extracted from Sloan Digital Sky Survey (SDSS) data release 7 and Baryon Oscillation Spectroscopic Survey (BOSS). We find that, for the both cases of using SN data alone and using SN+CMB+GC data, involving an additional parameter of β can reduce χ^2 by ~ 36 ; this shows that β deviates from a constant at 6σ confidence levels. Adopting SN+CMB+GC data, we find that compared to the constant β case, varying β yields a larger fractional matter density Ω_{m0} and a smaller reduced Hubble constant h ; moreover, varying β significantly increases the value of HDE model parameter c , leading to $c \approx 0.8$, consistent with the constraint results obtained before Planck. These results indicate that the evolution of β should be taken into account seriously in the cosmological fits. In addition, we find that relative to the differences between the constant β and varying $\beta(z)$ cases, the effects of different light-curve fitters on parameter estimation are very small.

PACS numbers: 98.80.-k, 98.80.Es, 95.36.+x

Keywords: Cosmological constraints, holographic dark energy, type Ia supernova, time-varying β

I. INTRODUCTION

Since its discovery, cosmic acceleration has become one of the most important research fields in modern cosmology [1–7]. Cosmic acceleration may be due to an unknown energy component (i.e., dark energy (DE) [8–21]), or a modification of general relativity (i.e., modified gravity (MG) [22–29]). For recent reviews, see, e.g., [30–39].

One of the most powerful probes of DE is the use of type Ia supernovae (SN Ia) [40–43]. In 2010, the Supernova Legacy Survey (SNLS) group released their three-years data, i.e. SNLS3 dataset [44]. Soon after, Conley et al. presented SN-only cosmological results by combining the SNLS3 SNe with various low- to mid- z samples [45], and Sullivan et al. presented the joint cosmological constraints by combining the SNLS3 dataset with other cosmological observations [46]. Depending on different light-curve fitters, Conley et al. [45] presented three SN data sets: “SALT2”, which consists of 473 SNe Ia; “SiFTO”, which consists of 468 SNe Ia; and “Combined”, which consists of 472 SNe Ia. Unlike other SN groups, the SNLS team treated two important quantities, stretch-luminosity parameter α and color-luminosity parameter β of SNe Ia, as free model parameters.

Currently, a critical challenge is the control of the systematic uncertainties of SNe Ia. One of the most important factors is the effect of potential SN evolution, i.e. the possibility for the redshift evolution of α and β . Current

studies show that α is still consistent with a constant, but the hints of evolution of β have been found in [47–51]. In [52], Mohlabeng and Ralston studied the case of Union2.1 sample using $\beta(z) = \beta_0 + \beta_1 z$, and found that β deviates from a constant at 7σ confidence levels (CL). In [53], using the SNLS3 data, Wang and Wang found that β increases significantly with z at the 6σ CL when systematic uncertainties are taken into account; moreover, they proved that this conclusion is insensitive to the lightcurve fitter used to derive the SNLS3 sample, or the functional form of $\beta(z)$ [53]. Therefore, the evolution of β should be taken into account seriously in the cosmology fits.

It is clear that the evolution of β will have significant effects. In [54], using the Λ -cold-dark-matter (Λ CDM) model, the w CDM model, and the Chevallier-Polarski-Linder (CPL) model, Wang, Li, and Zhang showed that adding a parameter of β could significantly improve the fitting results; in addition, considering the evolution of β is helpful in reducing the tension between SN and other cosmological observations. It should be pointed out that all the models considered in [54] are very simple. To further study the issue of varying β , some more specific DE models need to be taken into account. In this paper, we study the effects of a time-varying β on parameter estimation in the holographic dark energy (HDE) model [55]. The HDE is a physically plausible DE candidate based on the holographic principle [56]; it has been widely studied both theoretically [57] and observationally [58].

We first briefly review the theoretical framework of the HDE model. In [59], Cohen *et al.* suggested that quantum zero-point energy of a system with size L should not exceed the mass of a black hole with the same size, i.e.,

*Corresponding author.

†Electronic address: zhangxin@mail.neu.edu.cn

$L^3 k_{\max}^4 \leq LM_{\text{Pl}}^2$ (here M_{Pl} is the reduced Planck mass, and k_{\max} is the ultraviolet (UV) cutoff of the system). Therefore, the UV cutoff of a system is related to its infrared (IR) cutoff. When we consider the whole universe, the vacuum energy related to this holographic principle can be viewed as dark energy, and the corresponding energy density becomes

$$\rho_{\text{de}} = 3c^2 M_{\text{Pl}}^2 L^{-2}, \quad (1)$$

where c is a dimensionless model parameter that modulates the DE density [55]. In [55], Li suggested that the IR length-scale cutoff should be chosen as the size of the future event horizon of the universe, $R_{\text{eh}}(t) = a(t) \int_t^{+\infty} dt'/a(t')$. More generically, when we also consider the spatial curvature in a universe, the IR length cut-off L takes the form

$$L = ar(t), \quad (2)$$

where

$$r(t) = \frac{1}{\sqrt{k}} \text{sinn} \left(\sqrt{k} \int_t^{+\infty} \frac{dt'}{a(t')} \right), \quad (3)$$

with $\text{sinn}(x) = \sin(x)$, x , and $\sinh(x)$ for $k > 0$, $k = 0$, and $k < 0$, respectively. This leads to the following equation of state (EOS) of DE,

$$w_{\text{de}}(z) = -\frac{1}{3} - \frac{2}{3} \sqrt{\frac{\Omega_{\text{de}}(z)}{c^2} + \Omega_k(z)}, \quad (4)$$

which can yield an accelerated universe. In Eq. (4), the function $\Omega_{\text{de}}(z)$ is determined by the following coupled differential equation system [60],

$$\frac{1}{E} \frac{dE}{dz} = -\frac{\Omega_{\text{de}}}{1+z} \left(\frac{\Omega_k - \Omega_r - 3}{2\Omega_{\text{de}}} + \frac{1}{2} + \sqrt{\frac{\Omega_{\text{de}}}{c^2} + \Omega_k} \right), \quad (5)$$

$$\frac{d\Omega_{\text{de}}}{dz} = -\frac{2\Omega_{\text{de}}(1 - \Omega_{\text{de}})}{1+z} \left(\sqrt{\frac{\Omega_{\text{de}}}{c^2} + \Omega_k} + \frac{1}{2} - \frac{\Omega_k - \Omega_r}{2(1 - \Omega_{\text{de}})} \right), \quad (6)$$

where $E(z) \equiv H(z)/H_0$ is the dimensionless Hubble expansion rate, $H_0 = 100h \text{ km s}^{-1} \text{ Mpc}^{-1}$ is the Hubble constant, $\Omega_k(z) = \Omega_{k0}(1+z)^2/E(z)^2$, and $\Omega_r(z) = \Omega_{r0}(1+z)^4/E(z)^2$. In addition, $\Omega_{r0} = \Omega_{m0}/(1+z_{\text{eq}})$, $z_{\text{eq}} = 2.5 \times 10^4 \Omega_{m0} h^2 (T_{\text{cmb}}/2.7 \text{ K})^{-4}$ (here we take $T_{\text{cmb}} = 2.7255 \text{ K}$). The initial conditions are $E(0) = 1$ and $\Omega_{\text{de}}(0) = 1 - \Omega_{m0} - \Omega_{k0} - \Omega_{r0}$. By numerically solving Eqs. (5) and (6), we can obtain the evolution of $E(z)$, which can be used to calculate all the observational quantities appearing in Sec. II.

In this paper, we explore the effects of varying β on the SNLS3 constraints of the HDE model. In addition to the SNLS3 data, we also use the Planck distance prior data [61], as well as the latest galaxy clustering (GC) data extracted from SDSS DR7 [62] and BOSS [63]. In

addition, we also study the effects of different light-curve fitters on parameter estimation.

We describe our method in Sec. II, present our results in Sec. III, and conclude in Sec. IV. In this paper, we assume today's scale factor $a_0 = 1$, thus the redshift $z = a^{-1} - 1$. The subscript “0” always indicates the present value of the corresponding quantity, and the natural units are used.

II. METHOD

In this section, we will introduce how to include the SNLS3 data into the χ^2 analysis.

The comoving distance to an object at redshift z is given by

$$r(z) = H_0^{-1} |\Omega_{k0}|^{-1/2} \text{sinn}[|\Omega_{k0}|^{1/2} \Gamma(z)], \quad (7)$$

where $\Gamma(z) = \int_0^z \frac{dz'}{E(z')}$, and $\text{sinn}(x) = \sin(x)$, x , $\sinh(x)$ for $\Omega_{k0} < 0$, $\Omega_{k0} = 0$, and $\Omega_{k0} > 0$ respectively.

SN Ia data give measurements of the luminosity distance $d_L(z)$ through that of the distance modulus of each SN:

$$\mu_0 \equiv m - M = 5 \log \left[\frac{d_L(z)}{\text{Mpc}} \right] + 25, \quad (8)$$

where m and M represent the apparent and absolute magnitude of an SN. Moreover, the luminosity distance $d_L(z) = (1+z)r(z)$.

Here we use the SNLS3 data set. As mentioned above, based on different light-curve fitters, three SN sets of SNLS3 are given, including “SALT2”, “SiFTO”, and “Combined”. To perform a comparative study, all these three sets will be used in this paper.

In [53], by considering three functional forms (linear case, quadratic case, and step function case), Wang and Wang showed that the evolutions of α and β are insensitive to functional form of α and β . So in this paper, we just adopt a constant α and a linear $\beta(z) = \beta_0 + \beta_1 z$. Now, the predicted magnitude of an SN becomes

$$m_{\text{mod}} = 5 \log_{10} \mathcal{D}_L(z|\mathbf{p}) - \alpha(s-1) + \beta(z)\mathcal{C} + \mathcal{M}, \quad (9)$$

where $\mathcal{D}_L(z|\mathbf{p})$ is the luminosity distance multiplied by H_0 for a given set of cosmological parameters $\{\mathbf{p}\}$, s is the stretch measure of the SN light curve shape, and \mathcal{C} is the color measure for the SN. \mathcal{M} is a nuisance parameter representing some combination of the absolute magnitude of a fiducial SN, M , and the Hubble constant, H_0 . It must be emphasized that, to include host-galaxy information in the cosmological fits, Conley et al. [45] split the SNLS3 sample based on host-galaxy stellar mass at $10^{10} M_{\odot}$, and \mathcal{M} is allowed to be different for the two samples. Therefore, unlike other SN samples, there are two values of \mathcal{M} , \mathcal{M}_1 and \mathcal{M}_2 , for the SNLS3 data (for more details, see Sections 3.2 and 5.8 of [45]). Moreover, Conley et al. removed \mathcal{M}_1 and

\mathcal{M}_2 from cosmological fits by analytically marginalizing over them (for more details, see Appendix C of [45], as well as the public code, which is available at <https://tspace.library.utoronto.ca/handle/1807/24512>). In this paper, we just follow the recipe of [45].

Since the time dilation part of the observed luminosity distance depends on the total redshift z_{hel} (special relativistic plus cosmological), we have

$$\mathcal{D}_L(z|\mathbf{s}) = c^{-1}H_0(1 + z_{\text{hel}})r(z|\mathbf{s}), \quad (10)$$

where z and z_{hel} are the CMB restframe and heliocentric redshifts of the SN.

For a set of N SNe with correlated errors, the χ^2 function is [45]

$$\chi_{SN}^2 = \Delta \mathbf{m}^T \cdot \mathbf{C}^{-1} \cdot \Delta \mathbf{m} \quad (11)$$

where $\Delta \mathbf{m} \equiv m_B - m_{\text{mod}}$ is a vector with N components, m_B is the rest-frame peak B-band magnitude of the SN, and \mathbf{C} is the $N \times N$ covariance matrix of the SN.

The total covariance matrix is [45]

$$\mathbf{C} = \mathbf{D}_{\text{stat}} + \mathbf{C}_{\text{stat}} + \mathbf{C}_{\text{sys}}, \quad (12)$$

with the diagonal part of the statistical uncertainty given by [45]

$$\begin{aligned} \mathbf{D}_{\text{stat},ii} = & \sigma_{m_B,i}^2 + \sigma_{\text{int}}^2 + \sigma_{\text{lensing}}^2 + \sigma_{\text{host correction}}^2 \\ & + \left[\frac{5(1+z_i)}{z_i(1+z_i/2)\ln 10} \right]^2 \sigma_{z,i}^2 \\ & + \alpha^2 \sigma_{s,i}^2 + \beta(z_i)^2 \sigma_{\mathcal{C},i}^2 \\ & + 2\alpha C_{m_B s,i} - 2\beta(z_i) C_{m_B \mathcal{C},i} \\ & - 2\alpha\beta(z_i) C_{s\mathcal{C},i}, \end{aligned} \quad (13)$$

where $C_{m_B s,i}$, $C_{m_B \mathcal{C},i}$, and $C_{s\mathcal{C},i}$ are the covariances between m_B , s , and \mathcal{C} for the i -th SN, $\beta_i = \beta(z_i)$ are the values of β for the i -th SN. Note also that $\sigma_{z,i}^2$ includes a peculiar velocity residual of 0.0005 (i.e., 150 km/s) added in quadrature [45]. Following [45], here we fix the intrinsic scatter σ_{int} to ensure that $\chi^2/\text{dof} = 1$. Varying σ_{int} could have a significant impact on parameter estimation, see [64] for details.

We define $\mathbf{V} \equiv \mathbf{C}_{\text{stat}} + \mathbf{C}_{\text{sys}}$, where \mathbf{C}_{stat} and \mathbf{C}_{sys} are the statistical and systematic covariance matrices, respectively. After treating β as a function of z , \mathbf{V} is given in the form,

$$\begin{aligned} \mathbf{V}_{ij} = & V_{0,ij} + \alpha^2 V_{a,ij} + \beta_i \beta_j V_{b,ij} \\ & + \alpha V_{0a,ij} + \alpha V_{0a,ji} \\ & - \beta_j V_{0b,ij} - \beta_i V_{0b,ji} \\ & - \alpha \beta_j V_{ab,ij} - \alpha \beta_i V_{ab,ji}. \end{aligned} \quad (14)$$

It must be stressed that, while V_0 , V_a , V_b , and V_{0a} are the same as the “normal” covariance matrices given by the SNLS data archive, V_{0b} , and V_{ab} are *not* the same as the ones given there. This is because the original matrices of SNLS3 are produced by assuming that β is constant. We

have used the V_{0b} and V_{ab} matrices for the “Combined” set that are applicable when varying $\beta(z)$ (A. Conley, private communication, 2013).

In addition, to break the degeneracy between various model parameters, we also use the Planck distance prior data [61], as well as the latest galaxy clustering (GC) data extracted from SDSS DR7 [62] and BOSS [63]. For details on including Planck and GC data into the χ^2 analysis, see Ref. [54]. Thus, the total χ^2 function is

$$\chi^2 = \chi_{SN}^2 + \chi_{CMB}^2 + \chi_{GC}^2. \quad (15)$$

III. RESULTS

We perform a Markov Chain Monte Carlo (MCMC) likelihood analysis [65] to obtain $\mathcal{O}(10^6)$ samples for each set of results presented in this paper. We assume flat priors for all the parameters, and allow ranges of the parameters wide enough such that further increasing the allowed ranges has no impact on the results. The chains typically have worst e-values (the variance(mean)/mean(variance) of 1/2 chains) much smaller than 0.01, indicating convergence.

In the following section, we will discuss the effects of varying β and different light-curve fitters on the SNLS3 constraints on the HDE model, respectively.

A. The effects of varying β

In this subsection, we discuss the effects of varying β . As mentioned previously, to explore the evolution of β , we study the case of constant α and linear $\beta(z) = \beta_0 + \beta_1 z$; for comparison, the case of constant α and constant β is also taken into account. For simplicity, here we only use the SN data from the “Combined” set.

• SN-only cases

Firstly, we discuss the results given by the SN data alone. Notice that the Hubble constant h has been marginalized during the χ^2 fitting process of SNe Ia, so for this case, we only need to consider six free parameters, including α , β_0 , β_1 , Ω_{m0} , c , and Ω_{k0} .

In Table I, we list the fitting results for various constant β and linear $\beta(z)$ cases, where only the SNLS3 SNe data are used. The most obvious feature of this table is that a varying β can significantly improve the fitting results of HDE model: adding a parameter of β can reduce the best-fit values of χ^2 by ~ 36 . Based on the Wilk’s theorem, 36 units of χ^2 is equivalent to a Gaussian fluctuation of 6σ . This means that for HDE model, the result of $\beta_1 = 0$ is ruled out at 6σ CL. This result is consistent with the cases of the Λ CDM, the w CDM, and the CPL models [54]. In addition, we find that for both the constant β and the linear $\beta(z)$ cases, using the SNe data alone will lead to unreasonable results of Ω_{m0} , c , and Ω_{k0} , inconsistent with the constraint results given

TABLE I: A comparison for the fitting results of constant β and linear $\beta(z)$ cases. Only the SN(Combined) data are used in the analysis.

Parameter	constant β case	linear $\beta(z)$ case
α	$1.433^{+0.100}_{-0.108}$	$1.417^{+0.099}_{-0.100}$
β_0	$3.262^{+0.105}_{-0.108}$	$1.429^{+0.358}_{-0.383}$
β_1	N/A	$5.142^{+1.069}_{-0.998}$
Ω_{m0}	$0.112^{+0.056}_{-0.056}$	$0.090^{+0.052}_{-0.054}$
c	$1.252^{+0.414}_{-0.434}$	$1.262^{+0.737}_{-0.533}$
Ω_{k0}	$0.090^{+0.247}_{-0.238}$	$0.343^{+0.199}_{-0.209}$
χ^2_{min}	419.579	383.560

by previous studies [66–69]. This implies that using SNe data alone cannot constrain the cosmological parameters well.

In addition, we also calculate the best-fit values of \mathcal{M}_1 and \mathcal{M}_2 for the SNe-only cases. For the constant β case, we get $\mathcal{M}_1 = 0.00206$ and $\mathcal{M}_2 = 0.01789$; for the linear $\beta(z)$ case, we obtain $\mathcal{M}_1 = -0.00032$ and $\mathcal{M}_2 = -0.00559$. We can see that adding a parameter β_1 will not significantly change the values of \mathcal{M}_1 and \mathcal{M}_2 . This shows that \mathcal{M} has no significant effects on the conclusion of β 's evolution.

In Fig. 1, using SNe data alone, we plot the joint 68% and 95% confidence contours for $\{\beta_0, \beta_1\}$ (top panel), and the 68%, 95%, and 97% confidence constraints for the evolution of $\beta(z)$ (bottom panel), for the linear $\beta(z)$ case. For comparison, we also show the best-fit result of the constant β case on the bottom panel. The top panel shows that $\beta_1 > 0$ at a high CL. In addition, there is a clear degeneracy between β_0 and β_1 , which may be due to the kinematic fact of fitting a linear function. The bottom panel shows that $\beta(z)$ rapidly increases with z . Moreover, comparing with the best-fit result of constant β case, we can see that β deviates from a constant at 6σ CL. It needs to be pointed out that the evolutionary behaviors of $\beta(z)$ depends on the SN samples used. In [52], Mohlabeng and Ralston found that, for the Union2.1 SN data, $\beta(z)$ decreases with z . It is of great significance to study why different SN data give different evolutionary behaviors of $\beta(z)$, and some numerical simulation studies may be required to solve this problem. We will study this issue in future work.

• SN+CMB+GC cases

Next, let us discuss the results given by the SN+CMB+GC data. It should be mentioned that, in order to use the Planck distance priors data, two new model parameters, h and ω_b , must be added.

In Table II, we make a comparison for the fitting results of constant β and linear $\beta(z)$ cases, where the SN(Combined)+CMB+GC data are used. Again, we see that adding a parameter of β can reduce the values of χ^2_{min} by ~ 36 . This result is also consistent with the cases of the Λ CDM, the w CDM, and the CPL models

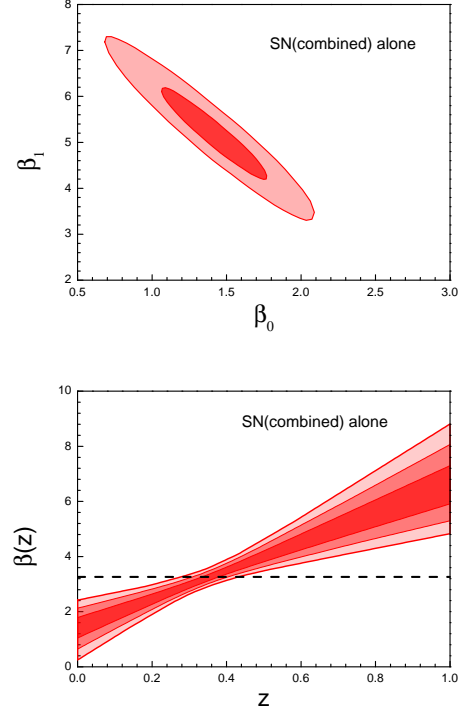


FIG. 1: The joint 68% and 95% confidence contours for $\{\beta_0, \beta_1\}$ (top panel) and the 68%, 95%, and 97% confidence constraints for $\beta(z)$ (bottom panel), given by the SN(Combined) data alone. For comparison, the best-fit result of constant β case is also shown in the bottom panel.

TABLE II: A comparison for the fitting results of constant β and linear $\beta(z)$ cases. The SN(Combined)+CMB+GC data are used in the analysis.

Parameter	constant β case	linear $\beta(z)$ case
α	$1.448^{+0.0760}_{-0.127}$	$1.416^{+0.097}_{-0.095}$
β_0	$3.270^{+0.082}_{-0.109}$	$1.403^{+0.359}_{-0.312}$
β_1	N/A	$5.167^{+0.971}_{-0.967}$
Ω_{m0}	$0.274^{+0.012}_{-0.016}$	$0.288^{+0.015}_{-0.013}$
h	$0.715^{+0.021}_{-0.014}$	$0.698^{+0.017}_{-0.017}$
c	$0.687^{+0.057}_{-0.068}$	$0.768^{+0.112}_{-0.068}$
ω_b	$0.02232^{+0.00025}_{-0.00030}$	$0.02230^{+0.00027}_{-0.00029}$
Ω_{k0}	$0.0077^{+0.0039}_{-0.0040}$	$0.0099^{+0.0051}_{-0.0037}$
χ^2_{min}	424.141	388.239

[54]. Therefore, we can conclude that the evolution of β is independent of the cosmological models in the background. This shows that the importance of considering β 's evolution in the cosmology fits. In addition, we find that after considering the observational data of CMB and GC, the parameter ranges of Ω_{m0} , c , and Ω_{k0} become much more reasonable.

We also calculate the best-fit values of \mathcal{M}_1 and \mathcal{M}_2 for the SN+CMB+GC cases. For the constant β case, we get $\mathcal{M}_1 = 0.00032$ and $\mathcal{M}_2 = -0.00251$; for the linear $\beta(z)$

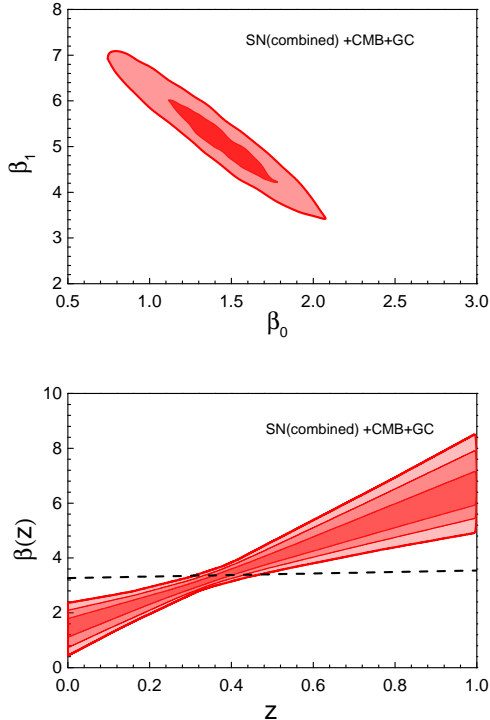


FIG. 2: The joint 68% and 95% confidence contours for $\{\beta_0, \beta_1\}$ (top panel) and the 68%, 95%, and 97% confidence constraints for $\beta(z)$ (bottom panel), given by the SN(Combined)+CMB+GC data. For comparison, the best-fit result of constant β case is also shown in the bottom panel.

case, we obtain $\mathcal{M}_1 = -0.00053$ and $\mathcal{M}_2 = -0.00599$. Again, we can see that \mathcal{M} has no significant effects on the conclusion of β 's evolution.

Let us discuss the effects of varying β with more details. In Fig. 2, using SN(combined)+CMB+GC data, we plot the joint 68% and 95% confidence contours for $\{\beta_0, \beta_1\}$ (top panel), and the 68%, 95%, and 97% confidence constraints for the reconstructed evolution of $\beta(z)$ (bottom panel), for the linear $\beta(z)$ case. For comparison, we also show the best-fit result of constant β case in the bottom panel. The top panel shows that $\beta_1 > 0$ at a high confidence level, while the bottom panel shows that $\beta(z)$ rapidly increases with z . In other words, according to this figure, we find the deviation of β from a constant at 6σ CL. This result is consistent with that of Refs. [53] and [54], and further confirms that the evolution of β is insensitive to the DE models and should be taken into account seriously in the cosmology fits.

In Fig. 3, using the same data, we plot the 1D marginalized probability distributions of Ω_{m0} , h , and c , for both the constant β and linear $\beta(z)$ cases. We find that varying β yields a larger Ω_{m0} , a smaller h , and a larger c .

It must be emphasized that the parameter c plays a very important role in determining the properties of HDE. For the cases of $c < 1$, $c = 1$, and $c > 1$,

the HDE corresponds to a phantom-type, an asymptotic Λ -type, and a quintessence-type DE, respectively. The previous studies showed that the best-fit value of this parameter is $c \simeq 0.7 - 0.8$. For examples, in [66], using the Gold04+WMAP+LSS data, Zhang and Wu gave $c = 0.81^{+0.23}_{-0.16}$; in [67], using the Constitution+WMAP5+SDSS data, Li et. al. got $c = 0.818^{+0.113}_{-0.097}$; in [68], using the Union2.1+WMAP7+BOSS data, Xu obtained $c = 0.750^{+0.0976}_{-0.0999}$. But in a later work [69], Li et. al. found that making use of the Planck data will significantly reduce the value of c ; for instance, using the Planck+WP+SNLS3+BAO+HST+lensing data, they obtained $c = 0.563 \pm 0.035$. In our paper, we find that, adding a parameter of β will significantly increase the value of c , and will lead to $c = 0.768^{+0.112}_{-0.068}$, which is consistent with those previous results obtained before the release of Planck data.

In Fig. 4, we plot the joint 68% and 95% confidence contours for $\{\Omega_{m0}, h\}$, $\{\Omega_{m0}, c\}$, and $\{c, h\}$. Again, we see that varying β yields a larger Ω_{m0} , a smaller h , and a larger c , compared to the case of assuming a constant β . Moreover, we also find that, for these two cases, the 2σ CL ranges of parameter space are quite different. This means that ignoring the evolution of β may cause systematic bias. In addition, it is clear that Ω_{m0} and h are strongly anti-correlated; this is also consistent with the cases of the Λ CDM, w CDM, and CPL models [54].

In Fig. 5, we plot the 68% confidence constraints for the reconstructed EOS $w(z)$ of HDE. From this figure, we see that varying β yields a larger $w(z)$: for the constant β case, $w(z=0) < -1$ at 1σ CL; while for the linear $\beta(z)$ case, $w(z=0)$ is still consistent with -1 at 1σ CL. Therefore, the results from varying β case are in better agreement with a cosmological constant than those from the constant β case.

B. The effects of different light-curve fitters

In this subsection, we discuss the effects of different light-curve fitters (including “Combined”, “SALT2”, and “SiFTO”). Notice that we also include the CMB and the GC data. For simplicity, here we only consider the case of linear $\beta(z)$. In Table III, we make a comparison for the fitting results given by the “Combined”, the “SALT2”, and the “SiFTO” SN sets. An obvious feature of this table is that the differences of various cosmological parameters are very small, while the differences of SN parameters (including α , β_0 and β_1) are a little larger. In the following section, we will discuss this issue with more details.

First, let us focus on the evolution of β . In Fig. 6, we plot the 68% confidence constraints for the reconstructed evolution of $\beta(z)$ in the HDE model, given by the “Combined”, the “SALT2”, and the “SiFTO” SN sets. It can be seen that the evolution of β given by the “Combined” set is very close to that given by the “SiFTO” SN set; in contrast, the “SALT2” set gives a different β 's evolution,

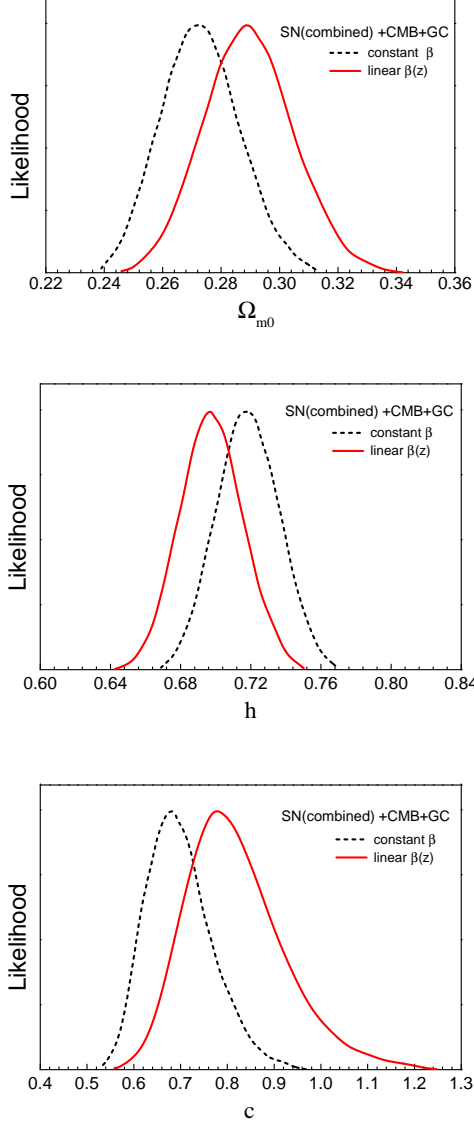


FIG. 3: The 1D marginalized probability distributions of Ω_{m0} (top panel), h (central panel), and c (bottom panel), given by the SN(Combined)+CMB+GC data. Both the results of constant β and linear $\beta(z)$ cases are presented.

TABLE III: A comparison for the fitting results given by the “Combined”, the “SALT2”, and the “SiFTO” SN sets. The linear $\beta(z)$ is adopted in the analysis.

Parameter	Combined	SALT2	SiFTO
α	$1.416^{+0.097}_{-0.095}$	$1.572^{+0.194}_{-0.151}$	$1.370^{+0.058}_{-0.081}$
β_0	$1.403^{+0.359}_{-0.312}$	$1.996^{+0.285}_{-0.249}$	$1.438^{+0.343}_{-0.359}$
β_1	$5.167^{+0.971}_{-0.967}$	$3.878^{+0.774}_{-0.835}$	$5.275^{+0.947}_{-0.894}$
Ω_{m0}	$0.288^{+0.015}_{-0.013}$	$0.285^{+0.017}_{-0.012}$	$0.284^{+0.018}_{-0.013}$
h	$0.698^{+0.017}_{-0.017}$	$0.701^{+0.017}_{-0.018}$	$0.702^{+0.017}_{-0.019}$
c	$0.768^{+0.112}_{-0.068}$	$0.751^{+0.081}_{-0.091}$	$0.745^{+0.105}_{-0.068}$
ω_b	$0.02230^{+0.00027}_{-0.00029}$	$0.02235^{+0.00023}_{-0.00033}$	$0.02233^{+0.00024}_{-0.00032}$
Ω_{k0}	$0.0099^{+0.0051}_{-0.0037}$	$0.0101^{+0.0040}_{-0.0043}$	$0.0091^{+0.0052}_{-0.0037}$

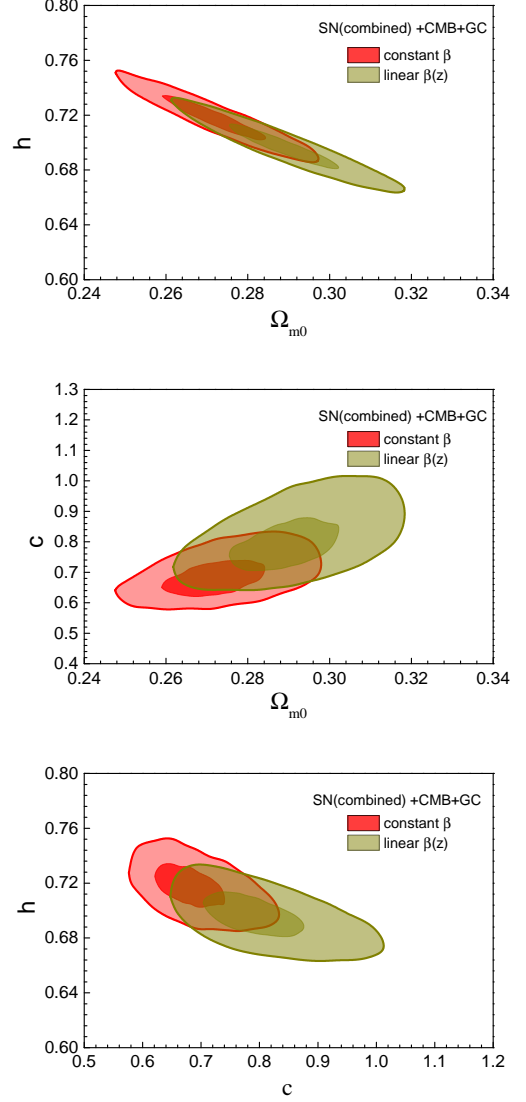


FIG. 4: The joint 68% and 95% confidence contours for $\{\Omega_{m0}, h\}$ (top panel), $\{\Omega_{m0}, c\}$ (central panel), and $\{c, h\}$ (bottom panel), given by the SN(Combined)+CMB+GC data. Both the results of constant β and linear $\beta(z)$ cases are presented.

whose increasing rate is a little smaller. But for all these three cases, the trends of $\beta(z)$ are still the same, and all of them deviate from a constant at a high CL. This result is consistent with the fixed cosmology background case (see Figure 5 of [53]). Thus, it further confirms that the evolution of β is insensitive to the light-curve fitters used to derive the SNLS3 sample.

Further, let us discuss the effects of different SNLS3 samples on parameter estimation. In Fig. 7, we plot the 1D marginalized probability distributions of Ω_{m0} , h , and c , given by the “Combined”, the “SALT2”, and the “SiFTO” SN sets. It can be seen that the results given by the “SALT2” and the “SiFTO” SN sets are very close, while the “Combined” set yields a larger Ω_{m0} , a smaller

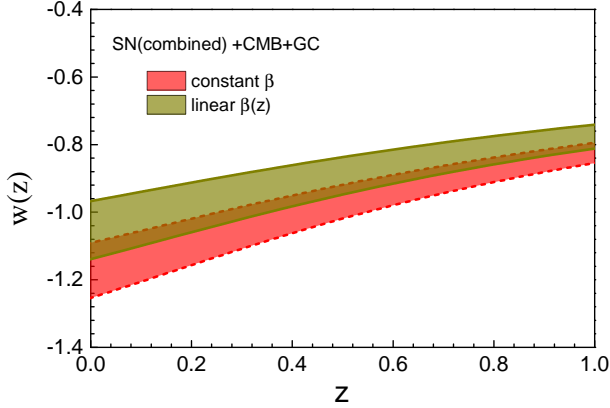


FIG. 5: The 68% confidence constraints for the EOS $w(z)$ of HDE, given by the SN(Combined)+CMB+GC data. Both the results of constant β and linear $\beta(z)$ cases are presented.

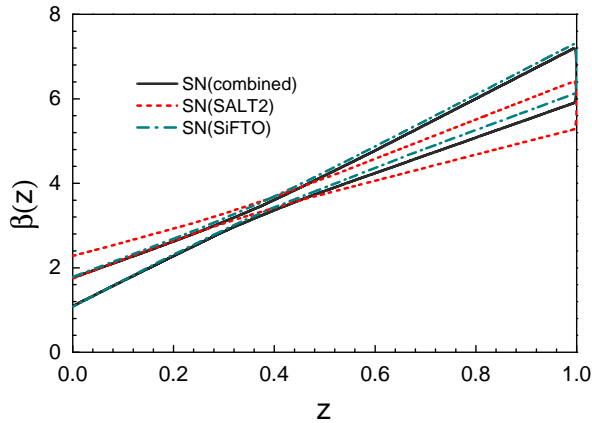


FIG. 6: The 68% confidence constraints for the evolution of $\beta(z)$ in the HDE model, given by the “combined”, the “SALT2”, and the “SiFTO” SN sets.

h , and a larger c . However, compared to the effects of varying β (see Fig. 3), the effects of different light-curve fitters are much smaller.

In Fig. 8, we plot the joint 68% and 95% confidence contours for $\{\Omega_{m0}, c\}$, given by the three SNLS3 samples. It is found that the results given by the “SALT2” and the “SiFTO” SN sets are very close, while the results given by the “combined” set are a little different. Moreover, compared to Fig. 4, it can be seen that the effects of different light-curve fitters are much smaller than those of varying β .

At last, we discuss the effects of different light-curve fitters on the EOS $w(z)$. In Fig. 9, we make a comparison for the 68% confidence constraints for the EOS $w(z)$ of HDE, given by the “Combined”, the “SALT2”, and the “SiFTO” SN sets. Again, we find that the results given by the “SALT2” and the “SiFTO” SN sets are very close;

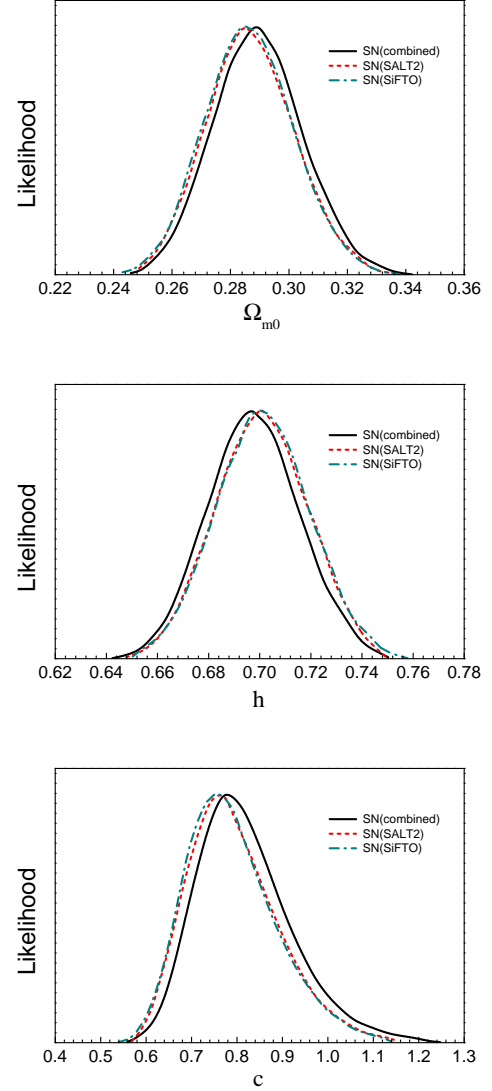


FIG. 7: The 1D marginalized probability distributions of Ω_{m0} (top panel), h (central panel), and c (bottom panel), given by the “combined”, the “SALT2”, and the “SiFTO” SN sets.

beside, the “Combined” set gives a larger $w(z)$. All these three SN sets yield a $w(z=0)$ that is consistent with -1 at 1σ CL. Compared to Fig. 5, again, we see that the effects of different light-curve fitters are much smaller.

Based on the results of Figs. 7, 8, and 9, we can conclude that compared to the differences between constant β and varying $\beta(z)$ cases, the effects of different light-curve fitters on parameter estimation are very small.

IV. DISCUSSION AND SUMMARY

It is well known that the systematic uncertainties of SNe Ia have become the key issue of SN cosmology. One of the most important systematic uncertainties for SNe

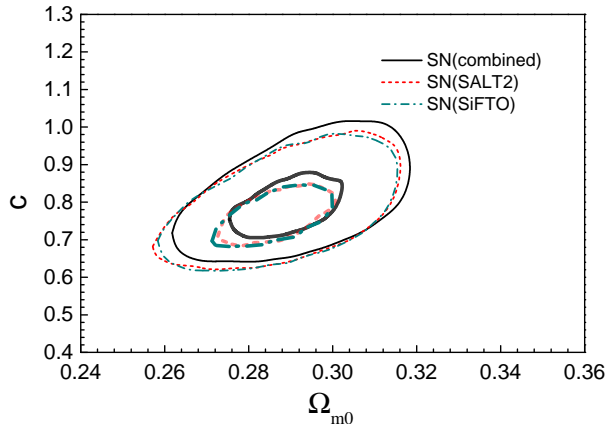


FIG. 8: The joint 68% and 95% confidence contours for $\{\Omega_{m0}, c\}$, given by the “combined”, the “SALT2”, and the “SiFTO” SN sets.

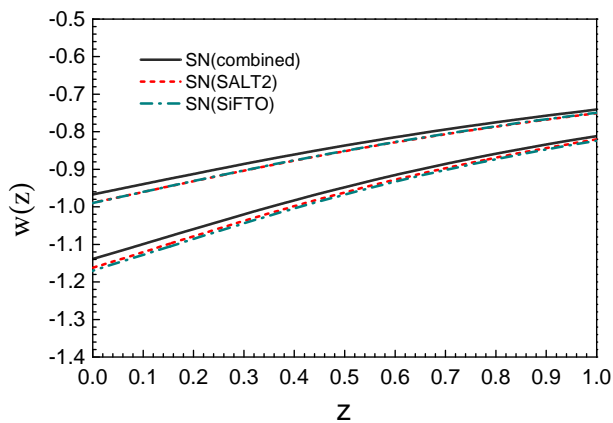


FIG. 9: The 68% confidence constraints for the EOS $w(z)$ of HDE, given by the “combined”, the “SALT2”, and the “SiFTO” SN sets.

Ia is the potential SN evolution, i.e., the possibility of the evolution of α and β with redshift z . In [53], Wang and Wang found that for the SNLS3 data there is strong evidence for the evolution of β . It must be emphasized that β ’s evolution was not only discovered in the SNLS3 sample, but also discovered in the other SN datasets (such as Pan-STARRS1 [51] and Union2.1 [52]). Therefore, it is not an isolated phenomenon, and should be taken into account very seriously.

It is clear that the evolution of β will have significant effects. In [54], using the Λ CDM model, the w CDM model, and the CPL model, Wang, Li, and Zhang showed that a time-varying β has significant impact on parameter estimation; besides, considering β ’s evolution is rather helpful for reducing the tension between supernova and other cosmological observations. To further study the issue of varying β , some more specific DE models need to be taken into account. This is the motivation of this work.

In this paper, we explored the effects of varying β on the cosmological constraints of HDE model. In addition to the SNLS3 data, we have also used the latest Planck distance priors data [61], as well as the latest GC data extracted from SDSS DR7 [62] and BOSS [63]. In addition, we have also studied the effects of different light-curve fitters on parameter estimation.

We found that for both the SNe alone and the SN+CMB+GC cases, adding a parameter of β can reduce the best-fit values of χ^2 of HDE model by ~ 36 (see Table I and Table II); it means that β deviates from a constant at the 6σ CL (see Figs. 1 and 2). This result is consistent with those of the Λ CDM, the w CDM, and the CPL models. This implies that the evolution of β is insensitive to the DE models in the background and should be taken into account seriously in the cosmology fits.

Adopting SN+CMB+GC data, we found that compared to the constant β case, varying β yields a larger Ω_{m0} and a smaller h (see Figs. 3); moreover, varying β will significantly increase the value of c , consistent with the constraint results obtained before the Planck data. In addition, for these two cases, the 2σ CL ranges of parameter space are quite different (see Figs. 4). This indicates that ignoring the evolution of β may causes systematic bias.

Varying β also yields a larger $w(z)$: for the constant β case, $w(z=0) < -1$ at 1σ CL; while for the linear $\beta(z)$ case, $w(z=0)$ is consistent with -1 at 1σ CL (see Fig. 5). So, the results from the varying β SN data are in better agreement with a cosmological constant than those from the constant β SN data.

We found that the evolution of β given by the “combined” and the “SiFTO” SN sets are very close; while the “SALT2” set will give a different β ’s evolution, whose increasing rate is a little smaller (see Fig. 6). We also found that the cosmology-fits results given by the “SALT2” and the “SiFTO” SN sets are very close, while the “Combined” set yields a larger Ω_{m0} , a smaller h , a larger c , and a larger $w(z)$ (see Figs. 7, 8 and 9). However, compared to the differences between constant β and time-varying $\beta(z)$ cases, the effects of different light-curve fitters are very small.

In this paper, only the potential SN evolution is taken into account. Some other factors, such as the evolution of σ_{int} [64], may also cause systematic uncertainties for SNe Ia. This issue deserves further study in the future.

Acknowledgments

We thank Yun-He Li for the helpful discussions. We are also grateful to Alex Conley for providing us with the SNLS3 covariance matrices that allow redshift-dependent α and β . We acknowledge the use of CosmoMC. SW is supported by the National Natural Science Foundation of China under Grant No. 11405024 and the Fundamental Research Funds for the Central Universities under

Grant No. N130305007. XZ is supported by the National Natural Science Foundation of China under Grant

No. 11175042 and the Fundamental Research Funds for the Central Universities under Grant No. N120505003.

-
- [1] Riess A G, Filippenko A V, Challis P, et al. Observational Evidence from Supernovae for an Accelerating Universe and a Cosmological Constant. *Astron J*, 1998, 116: 1009-1038; Perlmutter S, Aldering G, Goldhaber G, et al. Measurements of Omega and Lambda from 42 High-Redshift Supernovae. *Astrophys J*, 1999, 517: 565-586.
 - [2] Spergel D N, Verde L, Peiris H V, et al. First Year Wilkinson Microwave Anisotropy Probe (WMAP) Observations: Determination of Cosmological Parameters. *Astrophys J Suppl*, 2003, 148: 175-194; Bennet C L, Halpern M, Hinshaw G, et al. First Year Wilkinson Microwave Anisotropy Probe (WMAP) Observations: Preliminary Maps and Basic Results. *Astrophys J Suppl*, 2003, 148: 1-27; Spergel D N, Bean R, Dore O, et al. Wilkinson Microwave Anisotropy Probe (WMAP) Three Year Results: Implications for Cosmology. *Astrophys J Suppl*, 2007, 170: 377-408; Page L, Hinshaw G, Komatsu E, et al. Three Year Wilkinson Microwave Anisotropy Probe (WMAP) Observations: Polarization Analysis. *Astrophys J Suppl*, 2007, 170: 335-376; Hinshaw G, Nolta M R, Bennett C L, et al. Three-Year Wilkinson Microwave Anisotropy Probe (WMAP) Observations: Temperature Analysis. *Astrophys J Suppl*, 2007, 170: 288-334.
 - [3] Tegmark M, Strauss M, Blanton M, et al. Cosmological parameters from SDSS and WMAP. *Phys Rev D*, 2004, 69: 103501; Tegmark M, Blanton M, Strauss M, et al. The 3D power spectrum of galaxies from the SDSS. *Astrophys J*, 2004, 606: 702-740; Tegmark M, Eisenstein D, Strauss M, et al. Cosmological Constraints from the SDSS Luminous Red Galaxies. *Phys Rev D*, 2006, 74: 123507.
 - [4] Komatsu E, Dunkley J, Nolta M R, et al. Five-Year Wilkinson Microwave Anisotropy Probe (WMAP) Observations: Cosmological Interpretation. *Astrophys J Suppl*, 2009, 180: 330-376; Komatsu E, Smith K M, Dunkley J, et al. Seven-Year Wilkinson Microwave Anisotropy Probe (WMAP) Observations: Cosmological Interpretation. *Astrophys J Suppl*, 2011, 192: 18.
 - [5] Percival W J, Reid B A, Eisenstein D J, et al. Baryon Acoustic Oscillations in the Sloan Digital Sky Survey Data Release 7 Galaxy Sample. *Mon Not Roy Astron Soc*, 2010, 401: 2148-2168; Sanchez A G, Scoccola C G, Ross A J, et al. The clustering of galaxies in the SDSS-III Baryon Oscillation Spectroscopic Survey: cosmological implications of the large-scale two-point correlation function. *Mon Not Roy Astron Soc*, 2012, 425: 415-437.
 - [6] Drinkwater M, Jurek R J, Blake C, et al. The WiggleZ Dark Energy Survey: survey design and first data release. *Mon Not Roy Astron Soc*, 2010, 401: 1429-1452; Blake C, Kazin E A, Beutler F, et al. The WiggleZ Dark Energy Survey: mapping the distance-redshift relation with baryon acoustic oscillations. *Mon Not Roy Astron Soc*, 2011, 418: 1707-1724.
 - [7] Riess A G, Macri L, Casertano S, et al. A 3% Solution: Determination of the Hubble Constant with the Hubble Space Telescope and Wide Field Camera 3. *Astrophys J*, 2011, 730: 119.
 - [8] Ratra B, Peebles P J E. Cosmology with a time-variable cosmological constant. *Astrophys J Lett* 1988, 325: 17; Caldwell R R, Dave R, Steinhardt P J. Cosmological Imprint of an Energy Component with General Equation of State. *Phys Rev Lett*, 1998, 80: 1582-1585; Zlatev I, Wang L, Steinhardt P J. Quintessence, Cosmic Coincidence, and the Cosmological Constant. *Phys Rev Lett*, 1999, 82: 896-899.
 - [9] Caldwell R R, A Phantom Menace? Cosmological consequences of a dark energy component with super-negative equation of state. *Phys Lett B*, 2002, 545: 23-29; Carroll S M, Hoffman M, Trodden M. Can the dark energy equation-of-state parameter w be less than -1 ? *Phys Rev D*, 2003, 68: 023509; Caldwell R R, Kamionkowski M, Weinberg N N. Phantom Energy and Cosmic Doomsday. *Phys Rev Lett*, 2003, 91: 071301.
 - [10] Armendariz-Picon C, Mukhanov V, Steinhardt P J. Essentials of k-essence. *Phys Rev D*, 2001, 63: 103510; Chiba T, Okabe T, Yamaguchi M. Kinetically driven quintessence. *Phys Rev D*, 2000, 62: 023511.
 - [11] Kamenshchik A Y, Moschella U, Pasquier V. An alternative to quintessence. *Phys Lett B*, 2001, 511: 265-268; Bento M C, Bertolami O, Sen A A. Generalized Chaplygin Gas, Accelerated Expansion and Dark Energy-Matter Unification. *Phys Rev D*, 2002, 66: 043507.
 - [12] Zhang X, Wu F Q, Zhang J. New generalized Chaplygin gas as a scheme for unification of dark energy and dark matter. *JCAP*, 2006, 01: 003; Liao K, Pan Y, Zhu Z H. Observational constraints on the new generalized Chaplygin gas model. *Res Astron Astrophys*, 2013, 13: 159.
 - [13] Padmanabhan T. Accelerated expansion of the universe driven by tachyonic matter. *Phys Rev D*, 2002, 66: 021301; Bagla J S, Jassal H K, Padmanabhan T. Cosmology with tachyon field as dark energy. *Phys Rev D*, 2003, 67: 063504.
 - [14] Wei H, Cai R G. Cosmological Evolution of Hesseence Dark Energy and Avoidance of the Big Rip. *Phys Rev D*, 2005, 72: 123507; Wei H, Tang N, Zhang S N. Reconstruction of Hesseence Dark Energy and the Latest Type Ia Supernovae Gold Dataset. *Phys Rev D*, 2007, 75: 043009.
 - [15] Zhao W, Zhang Y. The state equation of Yang-Mills field dark energy models. *Class Quant Grav*, 2006, 23: 3405; Xia T Y, Zhang Y. 2-loop Quantum Yang-Mills Condensate as Dark Energy. *Phys Lett B*, 2007, 656: 19; Wang S, Zhang Y, Xia T Y. 3-loop Yang-Mills Condensate Dark Energy Model And Its Cosmological Constraints. *JCAP*, 2008, 10: 037; Wang S, Zhang Y. Alleviation of Cosmic Age Problem In Interacting Dark Energy Model. *Phys Lett B*, 2008, 669: 201.
 - [16] Zhang X. Reconstructing holographic quintessence. *Phys Lett B*, 2007, 648: 1-7; Zhang X. Dynamical vacuum energy, holographic quintom, and the reconstruction of scalar-field dark energy. *Phys Rev D*, 2006, 74: 103505; Zhang J, Zhang X, Liu H. Holographic tachyon model.

- Phys Lett B, 2007, 651: 84-88; Zhang J, Zhang X, Liu H. Agegraphic dark energy as a quintessence. Eur Phys J C, 2008, 54: 303-309; Zhang X. Holographic Ricci dark energy: Current observational constraints, quintom feature, and the reconstruction of scalar-field dark energy. Phys Rev D, 2009, 79: 103509.
- [17] Zhang X. Coupled Quintessence in a Power-Law Case and the Cosmic Coincidence Problem. Mod Phys Lett A, 2005, 20: 2575; Zhang X. Statefinder diagnostic for coupled quintessence. Phys Lett B, 2005, 611: 1-7.
- [18] Freese K, Adams F C, Frieman J A, et al. Cosmology with decaying vacuum energy. Nucl Phys B, 1987, 287: 797-814; Frieman J A, Hill C T, Stebbins A, Waga I. Cosmology with Ultra-light Pseudo-Nambu-Goldstone Bosons. Phys Rev Lett, 1995, 75: 2077-2080; Chevallier M, Polarski D. Accelerating Universes With Scaling Dark Matter. Int J Mod Phys D, 2001, 10: 213-223; Linder E V. Exploring the Expansion History of the Universe. Phys Rev Lett, 2003, 90: 091301; Huterer D, Starkman G. Parameterization of Dark-Energy Properties: a Principal-Component Approach. Phys Rev Lett, 2003, 90: 031301; Huterer D, Cooray A. Uncorrelated Estimates of Dark Energy Evolution. Phys Rev D, 2005, 71: 023506; Shafieloo A, Sahni V, Starobinsky A A. Is cosmic acceleration slowing down? Phys Rev D, 2009, 80: 101301(R).
- [19] Wang Y, Tegmark M. New dark energy constraints from supernovae, microwave background and galaxy clustering. Phys Rev Lett, 2004, 92: 241302; Wang Y, Freese K. Probing Dark Energy Using Its Density Instead of Its Equation of State. Phys Lett B, 2006, 632: 449-452; Wang Y, Mukherjee P. Robust Dark Energy Constraints from Supernovae, Galaxy Clustering, and Three-Year Wilkinson Microwave Anisotropy Probe Observations. Astrophys J, 2006, 650: 1-6; Wang Y, Mukherjee P. Observational Constraints on Dark Energy and Cosmic Curvature. Phys Rev D, 2007, 76: 103533; Wang Y. Model-Independent Distance Measurements from Gamma-Ray Bursts and Constraints on Dark Energy. Phys Rev D, 2008, 78: 123532.
- [20] Wang Y, Tegmark M. Uncorrelated Measurements of the Cosmic Expansion History and Dark Energy from Supernovae. Phys Rev D, 2005, 71: 103513.
- [21] Huang Q G, Li M, Li X D, Wang S. Fitting the Constitution SNIa Data with Redshift Binned Parameterization Method. Phys Rev D, 2009, 80: 083515; Wang S, Li X D, Li M. Revisit of cosmic age problem. Phys Rev D, 2010, 82: 103006; Li M, Li X D, Zhang X. Comparison of dark energy models: A perspective from the latest observational data. Sci China Phys Mech Astron, 2010, 53: 1631-1645; Wang S, Li X D, Li M. Exploring the Latest Union2 SNIa Dataset by Using Model-Independent Parameterization Methods. Phys Rev D, 2011, 83: 023010; Li X D, Li S, Wang S, et al. Probing Cosmic Acceleration by Using the SNLS3 SNIa Dataset. JCAP, 2011, 07: 011; Ma J Z, Zhang X. Probing the dynamics of dark energy with novel parametrizations. Phys Lett B, 2011, 699: 233-238; Li H, Zhang X. Constraining dynamical dark energy with a divergence-free parametrization in the presence of spatial curvature and massive neutrinos. Phys Lett B, 2012, 713: 160-164; Li X D, Wang S, Huang Q G, et al. Dark Energy and Fate of the Universe. Sci China Phys Mech Astron, 2012, 55: 1330-1334; Zhang J F, Zhao L A, Zhang X. Revisiting the interacting model of new agegraphic dark energy. Sci China-Phys Mech Astron, 2014, 57: 387-392.
- [22] Sahni V, Habib S. Does Inflationary Particle Production Suggest $\Omega_m < 1$? Phys Rev Lett, 1998, 81: 1766.
- [23] Parker L, Raval A. Nonperturbative effects of vacuum energy on the recent expansion of the universe. Phys Rev D, 1999, 60: 063512.
- [24] Dvali G, Gabadadze G, Porrati M. 4D Gravity on a Brane in 5D Minkowski Space. Phys Lett B, 2000, 485: 208-214.
- [25] Nojiri S, Odintsov S D, Sasaki M. Gauss-Bonnet dark energy. Phys Rev D, 2005, 71: 123509.
- [26] Nicolis A, Rattazzi R, Trincherini E. The galileon as a local modification of gravity. Phys Rev D, 2009, 79: 064036.
- [27] Hu W, Sawicki I. Models of $f(R)$ Cosmic Acceleration that Evade Solar-System Tests. Phys Rev D, 2007, 76: 064004; Starobinsky A A. Disappearing cosmological constant in $f(R)$ gravity. J Exp Theor Phys Lett, 2007, 86: 157-163.
- [28] Bengochea G R, Ferraro R. Dark torsion as the cosmic speed-up. Phys Rev D, 2009, 79: 124019; Linder E V. Einstein's Other Gravity and the Acceleration of the Universe. Phys Rev D, 2010, 81: 127301.
- [29] Harko T, Lobo F S N, Nojiri S, Odintsov S D. $f(R, T)$ gravity. Phys Rev D, 2011, 84: 024020.
- [30] Copeland E J, Sami M, Tsujikawa S. Dynamics of dark energy. Int J Mod Phys D, 2006, 15: 1753-1936.
- [31] Frieman J, Turner M, Huterer D. Dark Energy and the Accelerating Universe. Ann Rev Astron Astrophys, 2008, 46: 385-432.
- [32] Linder E V. Mapping the Cosmological Expansion. Rept Prog Phys, 2008, 71: 056901.
- [33] Caldwell R R, Kamionkowski M. The Physics of Cosmic Acceleration. Ann Rev Nucl Part Sci, 2009, 59: 397-429.
- [34] Uzan J P. Tests of General Relativity on Astrophysical Scales. Gen Rel Grav, 2010, 42: 2219-2246.
- [35] Tsujikawa S. Dark energy: investigation and modeling. arXiv:1004.1493.
- [36] Nojiri S, Odintsov S D. Unified cosmic history in modified gravity: from $F(R)$ theory to Lorentz non-invariant models. Phys. Rept. 2011, 505: 59-144.
- [37] Li M, Li X D, Wang S, Wang Y. Dark Energy. Commun Theor Phys, 2011, 56: 525; Li M, Li X D, Wang S, Wang Y. Dark Energy. Universe, 2013, 1: 24.
- [38] Clifton T, Ferreira P G, Padilla A, Skordis C. Modified Gravity and Cosmology. Phys Rept, 2012, 513: 1-189.
- [39] Wang Y. Dark Energy. New York, Wiley-VCH 2010.
- [40] Kowalski M, Rubin D, Aldering G, et al. Improved Cosmological Constraints from New, Old and Combined Supernova Datasets. Astrophys J, 2008, 686: 749-778.
- [41] Hicken M, Michael Wood-Vasey W, Blondin S, et al. Improved Dark Energy Constraints from 100 New CfA Supernova Type Ia Light Curves. Astrophys J, 2009, 700: 1097-1140; Hicken M, Challis P, Jha S, et al. CfA3: 185 Type Ia Supernova Light Curves from the CfA. Astrophys J, 2009, 700: 331-357.
- [42] Amanullah R, Lidman C, Rubin D, et al. Spectra and Light Curves of Six Type Ia Supernovae at $0.511 < z < 1.12$ and the Union2 Compilation. Astrophys J, 2010, 716: 712-738.
- [43] Suzuki N, Rubin D, Lidman C, et al. The Hubble Space Telescope Cluster Supernova Survey: V. Improving the Dark Energy Constraints Above $z > 1$ and Building an Early-Type-Hosted Supernova Sample. Astrophys J, 2012, 746: 85.
- [44] Guy J, Sullivan M, Conley A, et al. The Supernova

- Legacy Survey 3-year sample: Type Ia Supernovae photometric distances and cosmological constraints. *Astron Astrophys*, 2010, 523: 7.
- [45] Conley A, Guy J, Sullivan M, et al. Supernova Constraints and Systematic Uncertainties from the First 3 Years of the Supernova Legacy Survey. *Astrophys J Suppl*, 2011, 192: 1.
- [46] Sullivan M, Guy J, Conley A, et al. SNLS3: Constraints on Dark Energy Combining the Supernova Legacy Survey Three Year Data with Other Probes. *Astrophys J*, 2011, 737: 102.
- [47] Astier P, Guy J, Regnault N, et al. The Supernova Legacy Survey: Measurement of Ω_M , Ω_Λ and w from the First Year Data Set. *Astron Astrophys*, 2006, 447: 31-48.
- [48] Kessler R, Becker A, Cinabro D, et al. First-year Sloan Digital Sky Survey-II (SDSS-II) Supernova Results: Hubble Diagram and Cosmological Parameters. *Astrophys J Suppl*, 2009, 185: 32-84.
- [49] Marriner J, Bernstein J P, Kessler R, et al. A More General Model for the Intrinsic Scatter in Type Ia Supernova Distance Moduli. *Astrophys J*, 2011, 740: 72.
- [50] Scolnic D, Riess A, Foley R J, et al. Color Dispersion and Milky-Way-like Reddening among Type Ia Supernovae. *Astrophys J*, 2014, 780: 37.
- [51] Scolnic D, Rest A, Riess A, et al. Systematic Uncertainties Associated with the Cosmological Analysis of the First Pan-STARRS1 Type Ia Supernova Sample. *Astrophys J*, 2014, 795: 1.
- [52] Muhlberg G, Ralston J. A Redshift Dependent Color-Luminosity Relation in Type Ia Supernovae. *Mon Not Roy Astron Soc*, 2014, 439: L16-L20.
- [53] Wang S, Wang Y. Exploring the Systematic Uncertainties of Type Ia Supernovae as Cosmological Probes. *Phys Rev D*, 2013, 88: 043511.
- [54] Wang S, Li Y H, Zhang X. Exploring the evolution of color-luminosity parameter β and its effects on parameter estimation. *Phys Rev D*, 2014, 89: 063524.
- [55] Li M. A model of holographic dark energy. *Phys Lett B*, 2004, 603: 1-5.
- [56] 't Hooft G. Dimensional Reduction in Quantum Gravity. gr-qc/9310026; Susskind L. The world as a hologram. *J Math Phys*, 1995, 36: 6377.
- [57] Horvat R. Holography and Variable Cosmological Constant. *Phys Rev D*, 2004, 70: 087301; Zhang X. Statefinder diagnostic for holographic dark energy model. *Int J Mod Phys D*, 2005, 14: 1597-1606; Pavon D, Zimdahl W. Holographic dark energy and cosmic coincidence. *Phys Lett B*, 2005, 628: 206-210; Setare M R. Interacting holographic dark energy model in non-flat universe. *Phys Lett B*, 2006, 642: 1-4; Horvat R, Pavon D. Constraining interacting dark energy models with flux destabilization. *Phys Lett B*, 2007, 653: 373-377; Chen B, Li M, Wang Y. Inflation with Holographic Dark Energy. *Nucl Phys B*, 2007, 774: 256-267; Zhang J, Zhang X, Liu H Y. Holographic dark energy in a cyclic universe. *Eur Phys J C*, 2007, 52: 693-699; Zhang J, Zhang X, Liu H Y. Statefinder diagnosis for the interacting model of holographic dark energy. *Phys Lett B*, 2008, 659: 26-33; Li M, Lin C S, Wang Y. Some issues concerning holographic dark energy. *JCAP*, 2008, 05: 023; Ma Y Z, Zhang X. Possible theoretical limits on holographic quintessence from weak gravity conjecture. *Phys Lett B*, 2008, 661: 239-245; Li M, Li X D, Lin C S, et al. Holographic Gas as Dark Energy. *Commun Theor Phys*, 2009, 51: 181-186; Nayak B, Singh L P. Present Acceleration of Universe, Holographic Dark Energy and Brans-Dicke Theory. *Mod Phys Lett A*, 2009, 24: 1785-1792; Kim K Y, Lee H W, Myung Y S. Density Perturbations in Decaying Holographic Dark Energy Models. *Mod Phys Lett A*, 2009, 24: 1267; Li M, Miao R X, Pang Y. Casimir Energy, Holographic Dark Energy and Electromagnetic Metamaterial Mimicking de Sitter. *Phys Lett B*, 2010, 689: 55-59; Li M, Wang Y. Quantum UV/IR Relations and Holographic Dark Energy from Entropic Force. *Phys Lett B*, 2010, 687: 243-247; Gong Y G, Li T J. A modified holographic dark energy model with infrared infinite extra dimension(s). *Phys Lett B* 2010, 683: 241-247; Zhang X. Heal the world: Avoiding the cosmic doomsday in the holographic dark energy model. *Phys Lett B* 2010, 683: 81-87.
- [58] Huang Q G, Gong Y G. Supernova Constraints on a holographic dark energy model. *JCAP*, 2004, 08: 006; Chang Z, Wu F Q, Zhang X. Constraints on holographic dark energy from X-ray gas mass fraction of galaxy clusters. *Phys Lett B*, 2006, 633: 14-18; Wang B, Lin C Y, Abdalla E. Constraints on the interacting holographic dark energy model. *Phys Lett B* 2006, 637: 357-361; Zhang X, Wu F Q. Constraints on Holographic Dark Energy from Latest Supernovae, Galaxy Clustering, and Cosmic Microwave Background Anisotropy Observations. *Phys Rev D*, 2007, 76: 023502; Nesseris S, Perivolaropoulos L. Tension and Systematics in the Gold06 SNIa Dataset. *JCAP*, 2007, 02: 025; Ma Y Z, Gong Y, Chen X L. Features of holographic dark energy under combined cosmological constraints. *Eur Phys J C*, 2009 60: 303-315; Li M, Li X D, Wang S, et al. Probing interaction and spatial curvature in the holographic dark energy model. *JCAP*, 2009, 12: 014; Zhang Z H, Li S, Li X D, et al. Revisit of the Interaction between Holographic Dark Energy and Dark Matter. *JCAP*, 2012, 06: 009.
- [59] Cohen A, Kaplan D, Nelson A. Effective Field Theory, Black Holes, and the Cosmological Constant. *Phys Rev Lett*, 1999, 82: 4971.
- [60] Li Y H, Wang S, Li X D, et al. Holographic dark energy in a universe with spatial curvature and massive neutrinos: a full Markov Chain Monte Carlo exploration. *JCAP*, 2013, 02: 033.
- [61] Wang Y, Wang S. Distance Priors from Planck and Dark Energy Constraints from Current Data. *Phys Rev D*, 2013, 88: 043522.
- [62] Chuang C H, Wang Y. Measurements of $H(z)$ and $D_A(z)$ from the Two-Dimensional Two-Point Correlation Function of Sloan Digital Sky Survey Luminous Red Galaxies. *Mon Not Roy Astron Soc*, 2012, 426: 226-236.
- [63] Chuang C H, Prada F, Cuesta A J, et al. The clustering of galaxies in the SDSS-III Baryon Oscillation Spectroscopic Survey: single-probe measurements and the strong power of normalized growth rate on constraining dark energy. *Mon Not Roy Astron Soc*, 2013, 433: 3559-3571.
- [64] Kim A. Type Ia Supernova Intrinsic Magnitude Dispersion and the Fitting of Cosmological Parameters. arXiv:1101.3513;
- [65] Lewis A, Bridle S. Cosmological parameters from CMB and other data: a Monte-Carlo approach. *Phys Rev D* 2002, 66: 103511.
- [66] Zhang X, Wu F Q. Constraints on holographic dark energy from type Ia supernova observations. *Phys Rev D*, 2005, 72: 043524.

- [67] Li M, Li X D, Wang S, et al. Holographic dark energy models: A comparison from the latest observational data. JCAP, 2009, 06: 036.
- [68] Xu L X. Constraints on the Holographic Dark Energy Model from Type Ia Supernovae, WMAP7, Baryon Acoustic Oscillation and Redshift-Space Distortion. Phys Rev D, 2013, 87: 043525.
- [69] Li M, Li X D, Ma Y Z, et al. Planck Constraints on Holographic Dark Energy. JCAP, 2013, 09: 021.